THE UNIVERSITY *of* EDINBURGH

Edinburgh Research Explorer

Prospects and applicability of wave energy for South Africa

OPEN ACCESS

Title Page

Manuscript: Prospects and Applicability of Wave Energy for South Africa

Corresponding author's email: g.lavidas@ed.ac.uk (George Lavidas)

Author: George Lavidas, Ph.D.
e-mail: g.lavidas@ed.ac.uk
Department: Institute for Energy Systems
Institution: University of Edinburgh, School of Engineering
Address: Colin MacLaurin Road, Edinburgh, EH9 3DW
Country of residence: 122 Rue de Stassart, Ixelles, 1050, Belgium
tel: +32 (0) 465 14 70 59
fax: +44 (0) 131 650 6554
Co-Author: Vengatesan Venugopal, Ph.D, CEng, FIMechE
e-mail: V.Venugopal@ed.ac.uk
Department: Institute for Energy Systems
Institution: University of Edinburgh, School of Engineering
Address: Colin MacLaurin Road, Edinburgh, EH9 3DW
Country of residence: Edinburgh, United Kingdom
Tel : +44 (0) 131 650 5652
Fax: +44 (0) 131 650 6554

Acknowledgements

ABSTRACT

Renewable energy offers significant opportunities for electricity diversification. South Africa belongs in developing nations and encompasses a lot of potential for renewable energy developments. Currently, majority of its electricity production originates from fossil fuels, incorporation of clean coal technologies will aid in reaching the assigned targets.

This study offers a long-term wave power quantification analysis with a numerical wave model. The investigation includes long-term resource assessment in the region, variability, seasonal and monthly wave energy content. Locations with high energy content but low variability, pose an opportunity that can contribute in the alleviation of energy poverty.

Application of wave converters depends on the combination of complex terms. The study presents resource levels and the joint distributions, which indicate suitability for converter selection. Depending on the region of interest, these characteristics change. Thus, this resource assessment adds knowledge on wave power, and optimal consideration for wave energy applicability.

1. Introduction

Recently the Conference of Parties (COP21) in Paris, reviewed and designated targets in the efforts of tackling Climate Change (United Nations, 2015). The significance of such an agreement signed by all participants cannot be stressed enough. Amongst the nations which signed the document and committed to the targets for Climate Change, was the developing nation of South Africa.

This agreement poses not only a challenge but also a significant opportunity for South Africa, to diversify and integrate renewable energy into its current power production mix. To date South Africa is heavily dependent on conventional fuels, such as coal. High dependence on fossil fuels has not provided stability to the region, and major power shortages are noticeable, with fear of increasing (Baker, Newell, & Phillips, 2014).

Another important factor that South Africa faces is its status as a developing country, expecting rise of its electricity demands in the near future. This will mean that the current energy poverty levels will also have to be alleviated, and wider grid connectivity will be required.

Early studies, have underlined the drawbacks and potential limitations at South Africa, underlying the fact that low levels of energy cost are not realistic. Currently, prices depend on a highly monopolised system of the operator/distributor and the State (Banks & Schaffler, 2006; Prasad & Visagie, 2005; Winkler, 2005).

While this study will not be concerned with the policy framework, and energy governmental affairs, it is important to point out the government vision and various studies. Who have envisaged a higher level for renewable energies (RE) in the country.

COP21 targets focus on climate prevention, renewable energy incorporation is vital for the development of country. With almost 92% from various fossil, 3% from nuclear and 5% from biomass, the opportunities for other renewable converters is high (Matekenya & Mehlwana, 2006; Szewczuk, 2009).

With no major installations of renewables, numerous studies have been produced over the year evaluating technical feasibility, and finances of renewable energy incorporation (Banks & Schaffler, 2006; Department of Energy, 2015; Prasad & Visagie, 2005). Most recent being (Department of Energy, 2015), represents the most up-to-date set

2

of proposals prior to the COP21 conference.

Primary focus of the deployment strategy is given on solar, wind and biomass potential of the country. Biomass currently has the highest RE contribution, due to the fact that it is widely used in rural areas i.e. wood pellets etc. Another, important technology with the possibility of massive development is solar. With focus on solar concentrator parks, solar water heater and photovoltaic parks. Though currently solar is not used in large scale installations, but rather by small communities and individual to provide some level of energy independence (Banks & Schaffler, 2006; Department of Energy, 2015).

Finally, wind is considered as a promising technology, with only recently having completed parts of resource mapping opportunities around South Africa, through the Wind Atlas of South Africa (WASA) (Department of Energy, 2015). Another attempt starting within 2016 for total mapping of the wind resource.

Amongst the considerations for development of technologies, is wave energy. With South Africa having over 900 Km of coastlines exposed to the South Hemisphere, and seas neighbouring the Atlantic and Indian Oceans. Potential of the resource is expected to provide substantial levels of clean electricity.

No designated studies exist towards the mapping, quantification and investigation of wave resource over the South African coastlines, although some level of information can be derived by various institutions, and previous studies which examined the global resource with oceanic models (Cornett, 2008; Gunn & Stock-Williams, 2012; B. Reguero, Losada, & Méndez, 2015; B. G. Reguero, Menéndez, Méndez, Mínguez, & Losada, 2012).

This resulted in trying to provide quantification of the wave resource in the region, with estimates ranging 20-50 MW/Km of coastline (Banks & Schaffler, 2006) with harvest potential around 56,800 GW (Prasad & Visagie, 2005). Other estimates claim that it could provide around 70 TWh/year (Banks & Schaffler, 2006).

Values such as the aforementioned, provide a positive picture on potential. However, limitations must be considered. Wave energy content in a region can be subdivided into three categories, deep water, intermediate depth and coastal (very shallow) waters.

The range of application by current WECs is expected to be within the depths of ≤ 150m (meaning coastal, and shore structures). Most studies, use larger oceanic models, that are highly efficient to compute and hindcast large regions. However, the same models are known for limitations concerning their abilities to resolve nearshore water equations (Janssen, 2008; Sartini, Mentaschi, & Besio, 2015). Since the wave energy is under future consideration, in-depth detail studies are required for coastal environments.

Within this study, we present a 18 years high resolution wave energy resource Atlas for the region. Specific considerations have been taken, in the construction of an appropriate model, temporal/spatial components resolution and physical processes.

The historical runs extend from 1st January 1998 at $00:00$ and reach up to 1st January 2015 at $00:00$. Numerous wave and wind parameters suitable not only for wave energy analysis, but any other source of climate study, have been collected every 1 hour. Both the gridded data (maps) and a wide selection of points is stored in $netCDF$ files to ensure proper storage and versatility of the subsequent database.

Following the calibration, validation and hindcast process, the resource is examined for its monthly, seasonal and annual. Interest is given to the potential energy and variability of the resource. Ensuring, that selection of the final additional location, for energy analysis, utilise a highly energetic resource but at the same time, exhibit the minimum amount of variation.

This extensive nearshore Atlas for the South African coasts, can provide significant information, assist in raising awareness, and promoting wave energy converters as potential contributors. The long-term nature of the data, ensure that the database we have developed includes highly spatial and temporal information of wave and spectral energy. Expanding our capabilities to local climate studies, nearshore sediment transports and extreme value analysis, though none of these is considered in this study.

2. Wave Model

The wave model used in this study, is the Simulating WAves Nearshore (SWAN) model (Delft, 2014a) version 41.01A. Since, the study is concerned with the coastal and nearshore resource, the use of SWAN can be considered as most appropriate (Booij, Ris, & Holthuijsen, 1999; Delft, 2014a; Janssen, 2008).

Differences of the model to other oceanic models (i.e.WAM, WaveWatch3), is its ability to enable and resolve coastal environments better (Bunney, 2011; Sartini et al., 2015; Venugopal et al., 2011). This is due to the inclusion of many physical options that are more appropriate for coastal and shallow water environments (Delft, 2014a).

In this study SWAN is used in a two-way nested mode, comprising of a coarse mesh of 0.25^o with coordinates -15 W to 60 E and -15 N to -60 S. And a inner finer mesh 0.041^o degrees from 16 W to 30 E and -30 N to -37 S, see Figure 1. The primary coarse mesh is used to provide subsequent boundary and spectral conditions for the finer assessments. In the first mesh no boundary conditions are given, thus the reason of selecting a larger domain, in order to ensure that the wave climate is properly resolved.

SWAN as any other numerical model requires specific considerations prior to an operational run. The use of ECMWF ERA-Interim winds was the wind input responsible for generation and propagation of the wave fields (ECMWF, 2014). The model run over a period of 18 years from 1998-2014, in a non-stationary mode with Spherical coordinates. The bathymetry data used in domain construction were obtained by ETOPO 1 (Amante & Eakins, 2014) and subsequently regular meshes were constructed.

The non-linear quadruplet interactions are resolved in a semi-implicit way per sweep, bottom friction is activated in both domains, with non-linear triad interaction Elderberky method using a proportional coefficient of 0.65, diffraction, bottom breaking, whitecaps, dissipation are also all activated.

Finally, to ensure stability of the solution algorithm a back-ward, back-time step is used, with desired convergence accuracy set at 99.9% and adjusted turning frequencies and directions coefficients. The frequency domain is subdivided into 30 bins, for both coarse and finer domains, with minimum frequency 0.035 Hz. The directional division is in Spherical coordinates and 24 bins, thus every 15°. While additional finer selections can be used, one has to account the increase in computational effort and equipment in contrast with the benefits.

2.1. *Calibration*

For the domain size, and its subsequent use, most important parameter that needs specific attention is the wind scheme. In order to enhance the selection of wind generation processes several different adjusted options were tested and appropriately quantified. Use of statistical quality indices such as correlation coefficients (R), model performance index (MPI), bias, Scatter Index (SI), standard deviations (STD), and statistics to con-

struct Taylor diagrams (Taylor, 2001), are used to assess the performance (Bowers, Morton, & Mould, 2000; EMEC, 2009; Ris, Holthuijsen, & Booij, 1999).

$$bias = \sum_{i=1}^{N} \frac{1}{N}(X_i - Y_i) \qquad (1)$$

$$rms = \sqrt{\frac{1}{N}\sum_{i=1}^{N}(X_i - Y_i)^2} \qquad (2)$$

$$R = \frac{\sum\limits_{i=1}^{N}((X_i - \overline{X_i})(Y_i - \overline{Y_i}))}{\sqrt{((\sum\limits_{i=1}^{N}((X_i - \overline{X_i})^2))((\sum\limits_{i=1}^{N}((Y_i - \overline{Y_i})^2))}} \qquad (3)$$

$$SI = \frac{rms}{\frac{1}{N}\sum\limits_{i=1}^{N} Y_i} \qquad (4)$$

$$MPI = |1 - \frac{rms}{rms_{change}}| \qquad (5)$$

$$rms_{change} = \sqrt{\frac{Y_i^2}{N}} \qquad (6)$$

where X_i is the simulated wave parameter, Y_i the buoy wave quantity, N measurements. The rms_{change} is similar to the use of rms but the data we take into consideration are only the observed. Use of several quantitative indices allows better classification, for example in some cases we may obtain a good bias, small SI and a moderate MPI. Thus, by incorporating more methods available, a correlation of the simulated and observed values can be established (Komen, Cavaleri, Donelan, Hasselmann, & Janssen, 1994; Ris et al., 1999). For these hindcasts the H_{sig}, T_{peak}, T_{m02} and $P_{k_{Dir}}$ are compared with all the buoy recorded values.

Calibration took into account different generation wind schemes, although some additional adjustments were considered. Firstly, all wind schemes do not account linear growth, thus an addition assignment of the linear growth coefficient was activated. This ensures to filter wave growth at frequencies lower that the Pierson-Moskowitz spectrum (Delft, 2014a).

First activated wind scheme is the WAM 3, which considers wind growth, based on a wind drag generation approach over thresholds of winds, hereby denoted as KOMEN (Komen et al., 1994). Second activated scheme is the WAM 4, which also accounts for wind growth. Between WAM3 and WAM4 there is a slight deviation in the estimates

of high frequency waves which are computed by a iterative method based on wind speeds. This method hereby is denoted as JANSSEN (Janssen, 1988, 1991). Third method is a wind growth scheme based on a non-linear saturation model based on Wu's wind formulation (Wu, 1982), hereby denoted as WESTH.

In all of the cases whitecaps have been activated and have been appropriately tuned, since every scheme has to account for different parametrisations (Delft, 2014b; Rogers, Hwang, & Wang, 2002; Zijlema, van Vledder, & Holthuijsen, 2012).

The benchmark year for the calibration was the year 2014, results have been validated with buoys provided by CSIR on behalf of the Transnet National Port Authority (TNPA) (CSIR, 2016). Table 1 presents the buoys which are selected for calibration.

Assessment of calibration is made through use of the proposed statistics seen in the Taylor diagram (Taylor, 2001). Which investigate the suitability of predicted/hindcast measurements over a recorded value (buoy). It measures and estimates the correlation, root-mean-square errors weighted by the sample number and the standard deviation of modelled parameters. Additional statistical practises have also been employed, such as Bias (Eq. 1), Scatter Index (SI) (Eq. 4), Model Performance Index (MPI) (Eq. 5). It has to be noted, that due to the resolution of coarser mesh the Mossel Bay location could not be represented.

The annual buoy measurement of 2014 are considered as the benchmark data, missing intervals having being processes and replaced by NaN (Not A Number) and have not been considered. Since there is no such thing as a "perfect" model (Taylor, 2001), the wide variety of indices and the visual confirmation of the generated hidncast are the tools used for the selection of most appropriate solution. The final decision is based on subjective terms by the user, assisted by statistical analysis. Models configurations whose calibration results show high similarity, the user has to decide on the desired configuration.

First location examined is the East London, located at the South East of the South African peninsula. Biases for the models are in favour of the KOMEN scheme with small bias of -0.006m. JANSSEN has a bias of -0.16m and WESTH -0.39m. Standard deviation is lower for WESTH followed by KOMEN, while RMSE is lowest for WESTH with similar levels for the other two schemes, see Fig. 2. Highest correlation is encountered in WESTH. Although the measurements show a better performance in "phase" for the JANSSEN scheme, see also Fig. 2.In all cases the MPI is at 0.95, while the scattering is less in KOMEN 0.20, followed by JANSSEN 0.22 and WESTH 0.28.

Concerning the periods, bias is smaller for KOMEN with -0.58 sec, JANSSEN -1.81 sec and WESTH -1.79 sec. With similar distribution of the RMSE KOMEN smallest and JANSSEN highest. Scattering of periods is 0.18 for KOMEN, 0.24 for JANSSEN and 0.23 for WESTH.

Examination of Fig. 2, shows that although the hindcasts have a good generation trend associated with the MPI index, WESTH presents the highest under-estimation of events. See for example the models performance between August and September (2000-2250). KOMEN and JANSSEN have reproduced well H_{sig} both in magnitude and generation trend, WESTH exhibits higher under-estimations.

Second location is the Saldanha Bay which is located in the South West of the South African peninsula at depth of 23 meters. Starting with the biases all schemes provide some over-estimation on H_{sig}, WESTH gives the least bias with 0.16m, followed by JANSSEN 0.35m, surprisingly KOMEN scheme displays the lowest performance 0.57m. The KOMEN solution produces constant over-prediction for all timesteps, while WESTH offers the best correspondence. Generation trend is similar for all models, though significant changes in magnitude exist, see Fig. 3.

Correlation is similar for all models, see Fig. 3, approximately at 0.83 for all solutions. RMSEs present similar values for KOMEN and JANSSEN 0.30 to 0.31m while WESTH shows the least with 0.28m, see also Fig. 3.

For this location two scenarios can be deemed as favourable, WESTH and JANSSEN. Between the two, WESTH has lowest RMSE and standard deviation, JANSSEN has close deviation values and slightly better correlation. It also manages to represent the peak values magnitude in better accordance, as seen in Fig. 3 for example between the measurement at 1750-2000 timesteps. The scatter index values are greater for KOMEN over 0.40, JANSSEN has 0.35 and WESTH the smallest with 0.26.

The behaviour of the periods are also examined. For the peak period component KOMEN produces the smallest biases with an under-estimation of -1.27 sec, while JANSSEN and WESTH record higher under-estimations at -2.74 and -2.6 sec respectively. This results in lowered scattering for the peak period hindcast of KOMEN at 0.19, 0.30 for JANSSEN and 0.27 for WESTH.

Standard deviations has the best performance for KOMEN 1.63 sec followed by WESTH 1.87sec, JANSSEN has a value of 2.3sec. RMSE is higher for JANSSEN at 2.55 sec and 0.4 seconds for the other solutions.

For mean zero crossing, T_{m02}, the highest correlation is given by KOMEN 0.72 followed by WESTH 0.69 and JANSSEN 0.64. RMSE display a similar behaviour as the peak period with JANSSEN under-performing and having a difference of 0.2sec in comparison with the other two schemes which have 1sec values. The scatter index is at 0.16 for KOMEN, 0.22 for JANSSEN and 0.21 for WESTH. The biases are 0.25, -1.08 and -1.06 seconds respectively.

While both KOMEN and WESTH presented good generation trends, comparison between the different locations exhibited differences. The performance of KOMEN at the East quadrant provided highest accuracy in terms of bias. For the South West location, on the other hand KOMEN offered significant over-estimations with the model over-predicting.

In the South West side WESTH provided a good overlap of modelled and measured data, although its performance at the other location was the least favourable. JANSSEN scheme in both cases offered good magnitude representation and generation trend. All hindcast datasets were able to simulate the magnitude of large height waves. This is considered as added value since use of such a long-term dataset is not limited to wave resource estimates, but can be used for analysis of extreme value conditions. This means that by providing higher "peaks" equivalent to the ones measured (lower peak bias), the dataset can subsequently have future usages. Based on the statistical and short-term comparisons, the selected scheme for the 18 years hindcast (1998-2014) is the JANSSEN scheme. The final database of both coarse and fine domains have a 1 hour time resolution outputs for all wave quantities and maps.

2.2. *Validation*

After the calibration and selection of suitable scheme, the model was run in a two-nested configuration. The final outputs from the fine domain are used to validate the model. Buoy recordings provided by CSIR (2016) were used to validate results from the numerical model with the JANSSEN scheme, at 3 hour intervals for years 2013 and 2014. The locations used for validation are Mossel Bay and East London.

The nested domain yielded improvements in the East London location by reducing

the differences of measured and hindcast data. Both locations for the years 2013-2014, exhibit good agreement, see Table 2. It has to be noted that bias is lower at Mossel bay with consistent underestimation present at East London. The hindcast presents good agreement with slight under-estimations. These have to be considered throughout the study and explanation of results. Suggesting that levels of wave energy presented here, might have slight differences in comparison to measured wave data. For directional validation angular statistics have been considered [1].

3. Resource Atlas

The SWAN model run as presented in Section 2, in a two-way nesting mode. Each year run individually utilising a "warm-start" configuration to alleviated dis-continuity of data produced. This ensures that from the first measurement spectral and wave data correspond realistic sea states and do not encompass "warm-up" sections.

For the overall region each year is examined for its annual and seasonal wave energy resource. The division is done in four seasons, December (previous year)-January-February (DJF), March-April-May (MAM), June-July-August (JJA), September-October-November (SON). To ensure proper representation for 1998 initiation of the run was set in December 1997. Monthly variations are estimated for every month of the year and then averaged over the 18 year data to provide with the overall content. Additional locations were isolated and the examination of wave power resource is performed in annual and monthly terms. Both cases examined allow us to have a clearer picture of the resource levels available.

3.1. *Power Potential*

The resource estimated is based on the form of wave energy for irregular waves, since most devices are estimated for installation at depth $\leq 150m$ (Carbon Trust & AMEC, 2012). The energy contained within waves expressed, in W/m, which corresponds to the energy per crest unit length. In SWAN energy components are computed with a formulation appropriate for the realist representation of resource. Over the summation of very different wave numbers frequencies (f) and directions (θ).

$$P_x = \rho g \int \int C_{gx} E(f, \theta) df\, d\theta \qquad (7)$$

$$P_y = \rho g \int \int C_{gy} E(f, \theta) df\, d\theta \qquad (8)$$

where $E(f, \theta)$ the energy density spectrum over an x (longitude) y (latitude) system. C_g are the components of absolute group velocities, water density (ρ), g gravitational acceleration. Total wave power is estimated in kW/m:

$$P_{wave} = \sqrt{P_x^2 + P_y^2} \qquad (9)$$

Existing technologies, wave energy converters (WECs), utilise for power production

---

[1]NaN correspond to absent buoy recordings

either the energy period (T_e), peak period (T_{peak}), and zero-crossing period (T_{m02}). Recent discussions though have proposed a universal approach concerning the period used, more specifically proposing T_e as the most appropriate quantity (Ingram, Smith, Bittencourt-Ferreira, & Smith, 2011; Pascal, Molina, Torres, & Andreu Gonzalez, 2015).

From both domains the annual and seasonal resources are estimated, allowing quantification of mean resource levels for the whole dataset. Consequently, focus is given at wave energy levels and trends in coastal region, see Figure 4. In the overall coarse domain the predominant wave energy is originating from the South East swell components. The distribution and levels of wave energy are within 15-20 kW/m around the nearshore location, see Fig. 4.

In terms of wave energy levels available, see Fig. 4 and 5, higher resource levels originate from the South-East. Nearshore magnitudes are slightly higher for the South East African peninsula. The complex orography of the West side show a greater degree of turning coastlines, which increase the non-linear interactions reducing the wave power levels to 5-10 kW/m.

In Fig. 5 the final overall seasonal wave power content is presented. From the mean of all seasons, higher energy content is consistent seen throughout MAM and JJA months. Coastal locations have average resource from 10-25 kW/m, consistent with the location analysis.

For the outer-side at Cape Town peninsula, levels of most energetic months are above 20 kW/m (MAM-JJA) and 15 kW/m SON-DJF, with small seasonal deviations. The South East side benefits from Eastern swells and higher energy levels with highest seasons over 20-25 kW/m. During low energetic months resource levels drops approximately to 5-7 kW/m. Regions such as East London, Port Elisabeth, Durban and Mossel Bay show encouraging results.

From both the seasonal and annual energy investigation lower resources are found on the centre West near Velddrif and St. Helena's Bay, where coastlines enhance the breaking of waves, reducing the energy content.

Examination of wave energy levels hot-spots allow us to extract and use multiple additional locations that may be suitable for wave energy applications. These were selected by the final hindcast dataset of the fine resolution mesh. The fine mesh allows greater reach at coastal areas.

Thus apart from the buoy locations examined, additional points are extracted and utilised, see Table 3 and Fig. 6. The locations have been considered around the South African coastlines, in a spatially distributed manner, in order to characterise the overall region.

Distribution of wave power around the area is quite different than the one met in the Northern Hemisphere, this is due to the difference of climatic conditions met in the Southern Hemisphere (Stopa, Cheung, Tolman, & Chawla, 2013). The location of South African coastlines offer a higher power content over the summer months, due to the higher seasonally wind occurring in the region and differences in climate patterns for the North and South hemispheres.

Stopa et al. (2013) reported that significant wave heights are higher in the Southern Hemisphere for the $50 - 95^{th}$ percentiles, while magnitude of the 99th is similar to North and South Hemispheres. Vinoth and Young (2011) used altimeter data and estimated the 100 year return period of wave height (H_{100}), with different techniques in the estimations were used. The highest returns were located in the upper region of the North Atlantic and the lower belt of the Southern Hemisphere.

From such observations and current datasets, summer periods provide higher levels

of wave power. The one year annual data from buoys are divided into months to present the monthly wave power resource at each location, see Fig. 7 for the buoys.

For the additional locations (see Table 3) their energy content is examined. Distribution of locations is equally space around the coastline to provide a better representation of the opportunities that exist taking into account a longer time frame.

The range of mean energy content at the locations does not show significant variations, see Fig 8. Depending on the characteristics location, depth, surrounding coastlines the mean energy content is similar. However years 2002, 2007 show a higher resource. At the same time from 2007 onwards there is a higher mean wave energy trend for all sites.

The 99th percentile provides with information on the highest frequently met annual conditions, see Fig 9. As in the examination of mean wave power resource, in 2007-2011 there is a significant increase of the 99th percentile. Specifically the highest increase can be seen in Points 3,4,6, while a decrease in the percentiles occurs for Point 5. After 2012 all locations exhibit a decrease in highest percentile.

Apart from mean and percentile values, recorded maxima of wave energy are presented Fig 10. Highest amounts of energy are almost never utilised by wave energy converters (WEC), on the contrary such high level can increase potential damages. While examination cannot substitute a detail extreme events analysis, it provides with information concerning the mean versus maximum power. Desirably maxima events would not be significantly higher than the mean, indicating that potential return periods would not compromise future WEC installations Hagerman (2001).

From Figs. 8-9 Points 3 and 4 present the highest mean resource and percentile, though the most severe event between the two occurs at Point 3 in 2003, 2005, 2008, 2009, see Fig. 10. Point 6 has similar mean resource and maximum is significantly lower, indicating a good site selection. On the low end of the resource, lowest mean was recorded for Points 1-2, Point 2 has a consistent higher mean value by ≈ 4 kW/m annually. Here maximum occurrences hincasted are ≈ 25 kW/m in regards to Point 1.

The mean over maximum resource provides a ratio of severity for each of the locations, taking into account the highest energy content encountered. Desirably one would expect the ratio to be low, indicating that the site presents a mean content which is not endangered by severe effects.

Asides mean and max wave energy values, one has to assess the level of variation in the annual resource. Most favourable locations should be consider the ones which have the highest mean, see Fig 8 and the lower fluctuations annually. This ensures that the energy production will not be deviate much by large annual alterations.

The variability of wave power can be investigated, amongst other methods, by disseminating distribution over the domain for standard deviations (STD). Favourably low values of STD indicate closer resource to the mean, thus higher potential applicability for wave energy.

Highest STD, see Fig. 12 is presented for Point 3 which also has recorded the highest event, Fig. 10. Lower values are found for Points 1 and 5. In all instances values appear to have an increase after 2006, showing similar trends with mean wave power. The mean overall estimation based on the resource for 18 years is given Table 4. The mean monthly resource for each location, as discussed previously, is higher for the summer months, the overall hindcast monthly levels for each of the locations are presented in Figs. 13

3.2. *Applicability Considerations*

To enhance the decision selection of devices in the region further analysis of the resource is required. Current state-of-the-art wave energy converters are classified according to their operational principles, installed capacity and range of operation (Babarit et al., 2012). With wave power being dependent on the H_{sig} and periods (T_e, T_{peak}, T_{m02}), the device selection should be made based on the probabilities of occurrence for a site.

Investigating bivariate distributions of wave height and energy period, the percentage of occurrences allows for a initial dissemination and future selection of the most appropriate device in terms of operational conditions. This can be considered as a pre-feasibility investigation stage for converter selection. By properly coupling the available annual resource with a converter, potential energy estimates can be quantified.

Utilising the hindcast recordings, monthly distribution of wave energy for the locations are presented, accompanied with the corresponding bivariate distributions. The joint distributions of the overall dataset can be used for the selection/consideration of appropriate WECs. Examining the overall binned H_{sig} and T_e selection of a WEC can be made based on its operational characteristics and metocean events, ensuring the higher levels of performance.

The joint distribution use all 18 years of hindcasted parameters to examine the dominant seastates that occur at each location. The number of occurrences (number of recorded instances), are shown in each cell, see Fig. 14. Classification of every state corresponds to set interval of 1 sec (T_e) and 1 meter (H_{sig}). This can be reduced to 0.5 due to the amount of data within the dataset previous classification was chosen. Overall each locations contains over 149,000 hours of H_{sig} and T_e records. Alongside the examination of mean annual wave energy (P_{wave}), this analysis can assist in the selection of suitable WECs. Each WEC has unique own operational values, examples of which have been presented in Babarit et al. (2012); Silva, Rusu, and Soares (2013). South African coastlines appear to have a favourable range of operation for medium operating devices at low depths.

For Point 1 maximum wave height recorded was approximately 6 meters and maximum frequency 0.05 Hz. Majority of occurrences though suggest that selection of a WEC operating within 1-4 meters (H_{sig}) and 4-11 sec T_e would yield favourable year to year operation. At Point 2 dominant conditions are for slightly lower H_{sig} 0.5-3 m and T_e from 3-9 sec. Point 3-4 have similar trends favouring ranges of operation for 1-4 m and 3-11 sec. Points 5-6 do not have a continuous pattern within their range with majority of values clustered in low wave heights. Point 5 presents the highest number of instances for H_{sig} 1-4 m and T_e 3-10 sec, while Point 6 have a larger number occurring from 1-4 m and 3-12 sec.

This can be also observed by the probabilities of exceedance diagram for H_{sig} and P_{wave}, see Fig. 15. The P_{wave} of the diagram has been reduced to make it convenient to extract information. Points 3 and 6 have the highest content of wave energy while Point 2 and 5 have similar levels of resource, Point 1 has the lowest content. From the comparison of exceedance wave power, highest energy locations are Point 3 and Point 6, while located at different areas, exhibit high values of resource.

Based on available data the high resource of the South African coastlines can be easily accessed and utilised. From distribution of seastates favourable operation of wave energy converter would be 1-4 meters and 0.1-0.5 Hz (2-9 sec).

4. Discussion

Wave energy is a renewable energy form that poses an untapped resource, for the South African region. Several regions indicate that applicability of wave energy converters is feasible. Although, it is important to use resource assessment studies to enhance decision making.

With WECs being a novel renewable solution, it is of high importance that potential future device selection is based on dominant metocean characteristics. Identifying energetic areas, can provide significant advantages in estimating power production, determining cost of energy, and develop policy frameworks. As in the case of any emerging technology, there is a wide array of potential converters, which not are suitable for cost effective production. The resource assessment, contributes to disseminate the overwhelming choices in technology selection.

Even at this immature stage for WECs, their operational characteristics, if matched properly to resource can provide significant amounts of energy. Rusu and Onea (2016), used a numerical wave model and WEC power matrices assessing their energy contribution around high and low energy areas. Results, indicated that when matching the resource data correctly capacity factor can reach up to 31%. Similarly, Lavidas (2016) matched resource data to WECs and found that pending on location, characteristics, and WEC selection factor reach up to 27% in energetic areas, while in lower power region similar WEC have $\approx$ 10-15%. In addition, Luppa, Cavallaro, Foti, and Vicinanza (2015) proposed resource assessment data to be used for scaling converters to local resource, enhancing their capacity factors in some cases by 10%.

In monetary terms, WECs remain a capital intensive option. However, their associated learning curves indicate that there is a large margin for reduction (MacGillivray, Jeffrey, Winskel, & Bryden, 2014; Ocean, 2013). Application of wave energy can thus contribute not only to the energy mix but also to the local economy, since majority of works requires local development by adding up to 10 jobs/MW (Dalton & Lewis, 2011).

5. Conclusions

With electricity needs of South Africa expected to increase in forthcoming years, the ambitious program of the government and targets set at the recent COP21 conference. Development of renewable energies are expected to play a significant role for the country. Currently a detail map of wind and solar resource exists for the South African region, although the potential of untapped wave resource has not been yet investigated. Thus, in order to enhance and assist in the development of renewable energies, all local resource have to been thoroughly mapped and assessed.

A 18 year (1998-2014) wave energy resource assessment is presented in the study. Hindcast was performed and focused on the South African coastlines, allowing for presentating a thorough Wave Atlas, indicating "hot-spots" for potential wave energy applications.

An appropriate nearshore numerical model was utilised in a two-way nested mode, to hindcast the energy resource levels. The coarser mesh had a lower spatial resolution and was primarily used for the development of overall wave fields, that were subsequently used in the nested high-resolution domain.

The study investigated levels of wave energy, and presented a calibrated model, based on different parametrizations of wind evolution. The region was assessed in

terms of energy content for both nearshore and deep water locations. The intra-annual variability and trend for the resource was examined. Annual variations were also investigated by use of appropriate statistical indices, which indicated the available resource and variations.

The coarse mesh provided vital information in the identification of wave energy "hot-spot" locations, which were then extracted by the nested high-resolution mesh. The results show that the energy resource in the region is high, and potential location can be easily considered for renewable application. Nearshore energy content of the region is good even at low depths, ranging form 10-20 kW/m. Considering the low easily accessible depths and short coast distances, the results indicate promising conditions for offshore wave applications.

The hindcast evaluation indicated that the resource has increased, in energy content, since 2007 alongside with some increases in the standard deviation. At locations selected maximum wave heights overall of approximately 6-7 m were recorded, with the 99th percentiles being high for considering the operational depths.

Medium range operation WEC can be easily adapted to the area, which based on the long-term examination of the resource distribution in H_{sig} and T_e can deliver reliable power supply, with minimum interruptions. Thus the wave resource of the area can be consider significant and can be further utilised for studies on the applicability of wave energy applications. Even at low depths ($\leqslant$ 30 meters), the wave energy content underlines a lot of promise for the future development and consideration of WECs in the region.

Disclosure

The authors disclose no conflict of interest

References

Amante, C., & Eakins, B. (2014). *ETOPO1 1 Arc-Minute Global Relief Model: Procedures, Data Sources and Analysis. NOAA Technical Memorandum NESDIS NGDC-24.* Retrieved from http://maps.ngdc.noaa.gov/viewers/wcs-client/

Babarit, a., Hals, J., Muliawan, M., Kurniawan, A., Moan, T., & Krokstad, J. (2012, may). Numerical benchmarking study of a selection of wave energy converters. *Renew. Energy*, *41*, 44–63. Retrieved from http://linkinghub.elsevier.com/retrieve/pii/S0960148111005672 doi:

Baker, L., Newell, P., & Phillips, J. (2014). The Political Economy of Energy Transitions: The Case of South Africa. *New Polit. Econ.*, *19*(6), 791–818. Retrieved from http://www.tandfonline.com/doi/abs/10.1080/13563467.2013.849674 doi:

Banks, D., & Schaffler, J. (2006). *The potential contribution of renewable energy in South Africa (with cost informations)* (Tech. Rep. No. February).

Booij, N., Ris, R. C., & Holthuijsen, L. H. (1999). A third-generation wave model for coastal regions: 1. Model description and validation. *J. Geophys. Res.*, *104*(C4), 7649. Retrieved from http://doi.wiley.com/10.1029/98JC02622 doi:

Bowers, J., Morton, I., & Mould, G. (2000, feb). Directional statistics of the wind and waves. *Appl. Ocean Res.*, *22*(1), 13–30. Retrieved from http://linkinghub.elsevier.com/retrieve/pii/S0141118799000255 doi:

Bunney, C. (2011). *A High Resolution SWAN Model Assessment: North Norfolk to Humber* (Tech. Rep. No. July). MET Office. Retrieved from www.metoffice.gov.uk

Carbon Trust, & AMEC. (2012). *Carbon Trust Foreword to UK Wave Resource Study* . (Tech. Rep. No. October).

Cornett, A. M. (2008). A Global Wave Energy Resource Assessment. *Proc. Eighteenth Int. Offshore Polar Eng. Conf. Vancouver,BC,Canada July 6-11*, *8*, 318–326.

CSIR. (2016). *Counsil for Scientific and Industrial Research (CSIR).* Retrieved from `http://www.csir.co.za/`

Dalton, G., & Lewis, T. (2011). Metrics for measuring job creation by renewable energy technologies, using Ireland as a case study. *Renewable and Sustainable Energy Reviews*, *15*, 2123–2133. doi:

Delft, T. (2014a). *SWAN scientific documentation Cycle III version 41.01* (T. Delft, Ed.). Delft University of Technology Faculty of Civil Engineering and Geosciences Environmental Fluid Mechanics Section.

Delft, T. (2014b). *SWAN User Manual Cycle III version 41.01.* Delft, Nederlands: Delft University of Technology Faculty of Civil Engineering and Geosciences Environmental Fluid Mechanics Section.

Department of Energy, S. A. (2015). *State of Renewable Energy in South Africa* (Tech. Rep.). Department of Energy. Retrieved from `www.energy.gov.za`

ECMWF. (2014). *ERA Interim.* Retrieved from `http://www.ecmwf.int/`

EMEC. (2009). Assessment of Wave Energy Resource. *Renew. Energy*, 1–36. Retrieved from `www.emec.org.uk/standards/assessment-of-wave-energy-resource/`

Gunn, K., & Stock-Williams, C. (2012). Quantifying the global wave power resource. *Renew. Energy*, *44*, 296–304. Retrieved from `http://dx.doi.org/10.1016/j.renene.2012.01.101` doi:

Hagerman, G. (2001). Southern New England Wave Energy Resource Potential. In *Build. energy.*

Ingram, D., Smith, G., Bittencourt-Ferreira, C., & Smith, H. (2011). *EquiMar: Protocols for the Equitable Assessment of Marine Energy Converters* (No. 213380). doi:

Janssen, P. A. (1988). Wave - induced Stress and drag of air flow over sea waves.pdf. *J. Phys. Oceanogr.*, *19*(6), 745–754.

Janssen, P. A. (1991). Quasi-Linear theory of Wind-Wave Generation applied to wave forecasting. *J. Phys. Oceanogr.*, *6*, 1631–1642.

Janssen, P. A. (2008, mar). Progress in ocean wave forecasting. *J. Comput. Phys.*, *227*(7), 3572–3594. Retrieved from `http://linkinghub.elsevier.com/retrieve/pii/S0021999107001659` doi:

Komen, G., Cavaleri, L., Donelan, M., Hasselmann, S., & Janssen, P. (1994). *Dynamics and Modelling of Ocean waves.* Cambridge University Press. Retrieved from `www.cambridge.org/9780521470476`

Lavidas, G. (2016). *Wave Energy Resource Modelling and Energy Pattern Identification Using a Spectral Wave Model* (Ph.D Thesis). University of Edinburgh, Edinburgh.

Luppa, C., Cavallaro, L., Foti, E., & Vicinanza, D. (2015). Potential wave energy production by different wave energy converters around Sicily. *J. Renew. Sustain. Energy*, *7*(6), 061701. Retrieved from `http://scitation.aip.org/content/aip/journal/jrse/7/6/10.1063/1.4936397` doi:

MacGillivray, A., Jeffrey, H., Winskel, M., & Bryden, I. (2014). Innovation and cost reduction for marine renewable energy: A learning investment sensitivity analysis. *Technol. Forecast. Soc. Change*, *87*, 108–124. Retrieved from `http://dx.doi.org/10.1016/j.techfore.2013.11.005` doi:

Matekenya, W., & Mehlwana, M. (2006). Energy Technologies for Climate Change Mitigation - What Is Appropriate for Sa ? In *Ind. commerical use energy conf.*

Ocean, S. (2013). *Ocean Energy: Cost of Energy and Cost Reduction Opportunities* (Tech. Rep. No. May). Retrieved from `http://si-ocean.eu/en/upload/docs/WP3/CoE report 3_2 final.pdf`

Pascal, R., Molina, Torres, A., & Andreu Gonzalez, A. (2015). Going further than the scatter

diagram : tools for analysing the wave resource and classifying sites. In *Proc. 11th eur. wave tidal energy conf. 6-11th sept 2015, nantes, fr.* (pp. 5–12). Nantes.

Prasad, G., & Visagie, E. (2005). *Renewable energy technologies for poverty alleviation Initial assessment report : South Africa* (Tech. Rep. No. June). Cape Town: Energy Research Centre, University of Cape Town, South Africa.

Reguero, B., Losada, I., & Méndez, F. (2015). A global wave power resource and its seasonal, interannual and long-term variability. *Appl. Energy*, *148*, 366–380. Retrieved from `http://linkinghub.elsevier.com/retrieve/pii/S030626191500416X` doi:

Reguero, B. G., Menéndez, M., Méndez, F. J., Mínguez, R., & Losada, I. J. (2012). A Global Ocean Wave (GOW) calibrated reanalysis from 1948 onwards. *Coast. Eng.*, *65*, 38–55. Retrieved from `http://dx.doi.org/10.1016/j.coastaleng.2012.03.003` doi:

Ris, R. C., Holthuijsen, L. H., & Booij, N. (1999). A third-generation wave model for coastal regions: 2.Verification. , *104*, 7667–7681.

Rogers, W., Hwang, P., & Wang, W. (2002). Investigation of Wave Growth and Decay in the SWAN Model : Three Regional-Scale Applications. *Phys. Oceanogr.*, 366–389.

Rusu, E., & Onea, F. (2016). Estimation of the wave energy conversion efficiency in the Atlantic Ocean close to the European islands. *Renew. Energy*, *85*, 687–703. Retrieved from `http://dx.doi.org/10.1016/j.renene.2015.07.042` doi:

Sartini, L., Mentaschi, L., & Besio, G. (2015). Evaluating third generation wave spectral models performances in coastal areas . An application to Eastern Liguria. In *Ocean. 2015 ieee.*

Silva, D., Rusu, E., & Soares, C. G. (2013). Evaluation of various technologies for wave energy conversion in the portuguese nearshore. *Energies*, *6*, 1344–1364. doi:

Stopa, J. E., Cheung, K. F., Tolman, H. L., & Chawla, A. (2013, oct). Patterns and cycles in the Climate Forecast System Reanalysis wind and wave data. *Ocean Model.*, *70*, 207–220. Retrieved from `http://linkinghub.elsevier.com/retrieve/pii/S1463500312001503` doi:

Szewczuk, S. (2009). Distributed Generation Systems for South Africa Based on Renewable Energy Resources. In *Ises sol. world congr. 2009 renew. energy shap. our futur.* (pp. 1128–1137).

Taylor, K. E. (2001). Summarizing aspects of model performance in a single diagram. *J. Geophys. Res.*, *106*, 7183–7192.

United Nations. (2015). *Adoption of the Paris Agreement* (Vol. FCCC/CP/20; Tech. Rep. No. December). Paris: United Nations Framework Convention on Climate Change. Retrieved from `http://unfccc.int/resource/docs/2015/cop21/eng/l09r01.pdf`

Venugopal, V., Davey, T., Girard, F., Smith, H., Cavaleri, L., Bertotti, L., & Mauro, S. (2011). *Equitable testing and evaluation of Marine Energy Extraction Devices of Performance, Cost and Environmental Impact. Deliverable 2.4 Wave Model Intercomparison* (Tech. Rep.).

Vinoth, J., & Young, I. R. (2011, mar). Global Estimates of Extreme Wind Speed and Wave Height. *J. Clim.*, *24*(6), 1647–1665. Retrieved from `http://journals.ametsoc.org/doi/abs/10.1175/2010JCLI3680.1` doi:

Winkler, H. (2005). Renewable energy policy in South Africa: policy options for renewable electricity. *Energy Policy*, *33*(1), 27–38. Retrieved from `http://linkinghub.elsevier.com/retrieve/pii/S0301421503001952` doi:

Wu, J. (1982). Wind-Stress Over Sea Surface From Breeze to Hurricane. *J. Geophys. Res.*, *87*(12), 9704–9706.

Zijlema, M., van Vledder, G., & Holthuijsen, L. (2012, jul). Bottom friction and wind drag for wave models. *Coast. Eng.*, *65*, 19–26. Retrieved from `http://linkinghub.elsevier.com/retrieve/pii/S0378383912000440` doi:

Tables

Table 1.: Buoy locations provided by CSIR (2016)

Location	Longitude	Latitude	Depth
East London	$29^o93^"$ East	$-33^o0.38^"$ South	27 meter
Saldanha Bay	$17^o97^"$ East	$-33^o0.5^"$ South	23 meter
Mossel Bay	$22^o15^"$ East	$-34^o12^"$ South	24 meter

Table 2.: Validation (H_{sig} in meters, T_{peak}, T_{m02} in seconds, and $P_{k_{Dir}}$ in degrees)

	East London 2013				East London 2014			
	H_{sig}	T_{peak}	T_{m02}	Pk_{Dir}	H_{sig}	T_{peak}	T_{m02}	Pk_{Dir}
RMSE	0.25	2.97	NaN	51.30	0.35	2.26	NaN	50.11
MPI	0.90	0.31	NaN	0.10	0.98	0.85	NaN	0.97
Av.Buoy	1.54	10.86	NaN	163.45	1.85	11.3	NaN	166.77
Av.SWAN	1.46	8.80	NaN	164.22	1.7	9.7	NaN	166.52
Bias	-0.08	-2.06	NaN	0.76	-0.15	-1.6	NaN	0.24
SI	0.16	0.27	NaN	0.31	0.19	0.20	NaN	0.30
	Mossel Bay 2013				Mossel bay 2014			
	H_{sig}	T_{peak}	T_{m02}	Pk_{Dir}	H_{sig}	T_{peak}	T_{m02}	Pk_{Dir}
RMSE	0.27	3.21	0.88	NaN	0.30	2.91	1.46	NaN
MPI	0.92	0.34	0.64	NaN	0.97	0.78	0.87	NaN
Av.Buoy	1.13	10.27	5.63	NaN	1.22	11.60	6.89	NaN
Av.SWAN	1.07	8.49	5.20	NaN	1.21	9.75	6.22	NaN
Bias	-0.05	-1.78	-0.42	NaN	-0.01	-1.85	-0.66	NaN
SI	0.24	0.31	0.15	NaN	0.24	0.25	0.21	NaN

Table 3.: Additional location Coordinates

Location	Longitude	Latitude	Depth
Point 1	$18^o13^"$ East	$-31^o88^"$ South	45 meter
Point 2	$17^o79^"$ East	$-32^o83^"$ South	43 meter
Point 3	$20^o04^"$ East	$-34^o88^"$ South	30 meter
Point 4	$21^o71^"$ East	$-34^o46^"$ South	50 meter
Point 5	$27^o88^"$ East	$-33^o13^"$ South	85 meter
Point 6	$25^o71^"$ East	$-34^o08^"$ South	89 meter

Table 4.: Mean Wave Power Resource for the hindcast

Location	Mean Resource (kW/m)	$\frac{P_{mean}}{P_{max}}$	STD	$99^{th} Percentile$
Point1	9.29	0.10	9.80	47.32
Point2	12.33	0.10	12.64	61.80
Point3	18.51	0.10	18.28	90.91
Point4	16.22	0.10	16.07	81.30
Point5	14.35	0.12	12.01	64.74
Point6	18.64	0.11	17.12	90.63

Figures

(1) Domains and meters depth, along the areas of investigation
(2) Taylor diagram for East London and comparison of the generated H_{sig} by the models, blue is the buoy measurements while the colours indicate results by each different scheme. The measurements are taken every 3 hours
(3) Taylor diagram for Saldanha Bay and comparison of the generated H_{sig} by the models, blue is the buoy measurements while the colours indicate the results by each different scheme. The measurements are taken every 3 hours
(4) Overall Wave Energy (kW/m) over the 18 years period (nested domain)
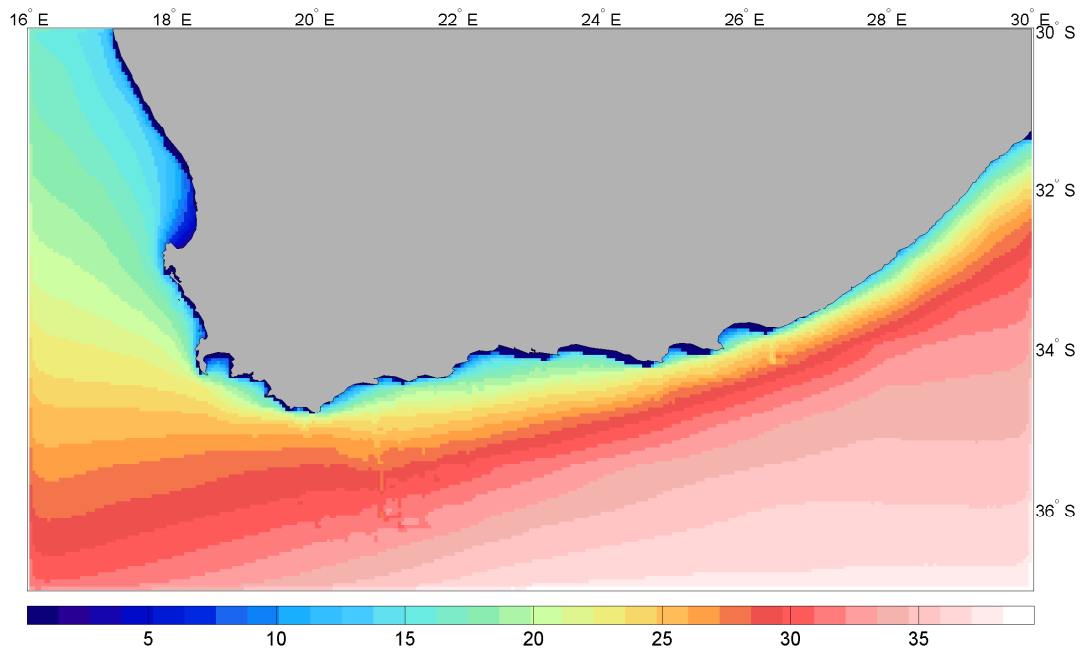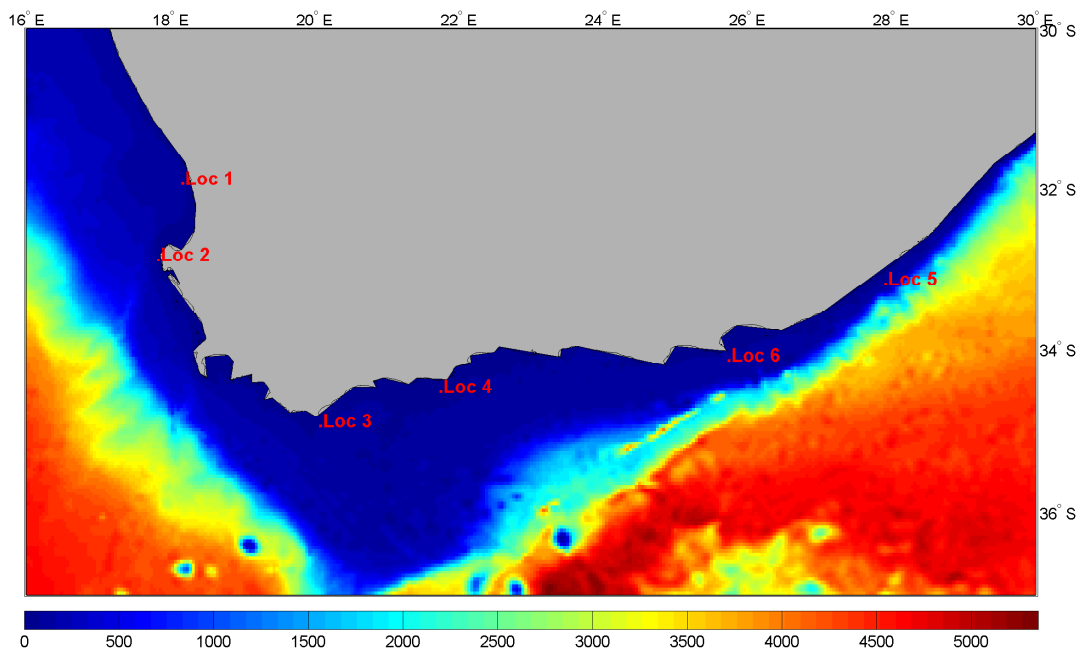(5) Seasonal Wave Power distribution
(6) Additional Locations Extracted, with corresponding depth (m)
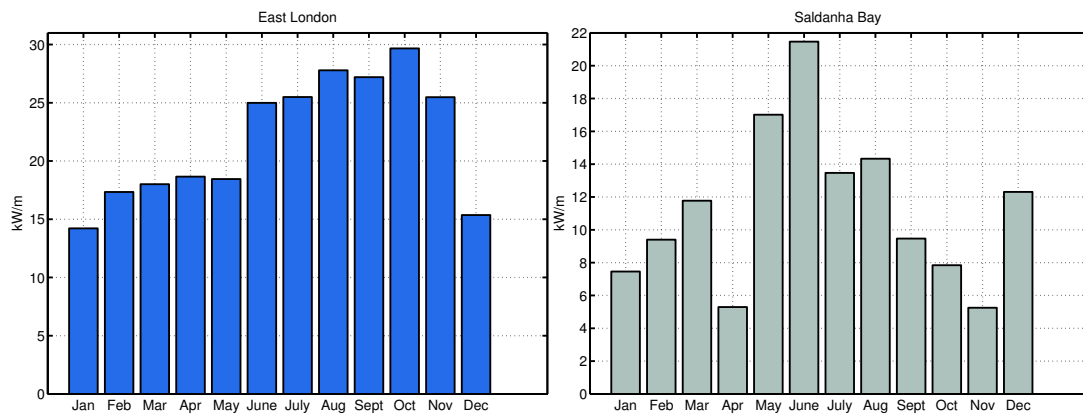(7) East London (left panel), Saldanha Bay (right panel) monthly measured wave power from the 2014 recordings by the buoy.
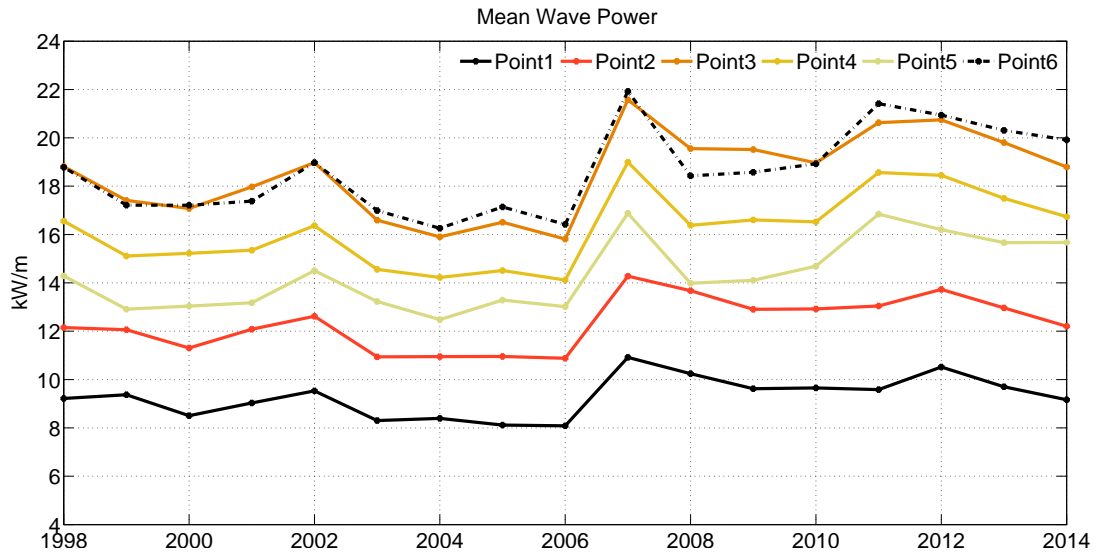(8) Annual Mean Wave Power
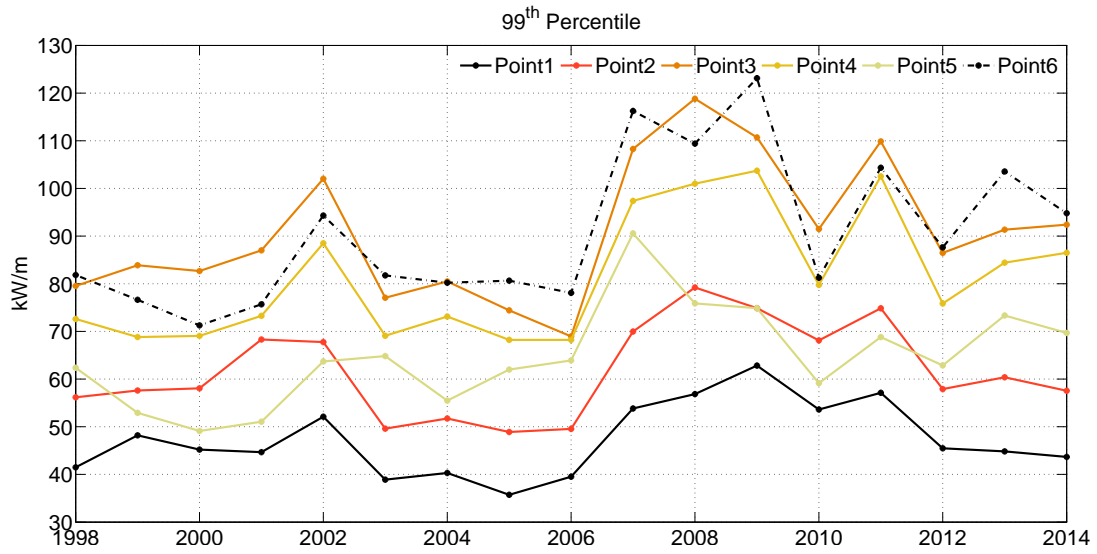(9) 99th percentiles for the locations
(10) Annual Maximum Wave Power Occurrence
(11) Mean Over Maximum encountered power levels
(12) Standard deviation
(13) Monthly Wave Power (kW/m) Estimates
(14) Bivariate H_{sig}-T_e for Point 1
(15) Exceedance Probabilities
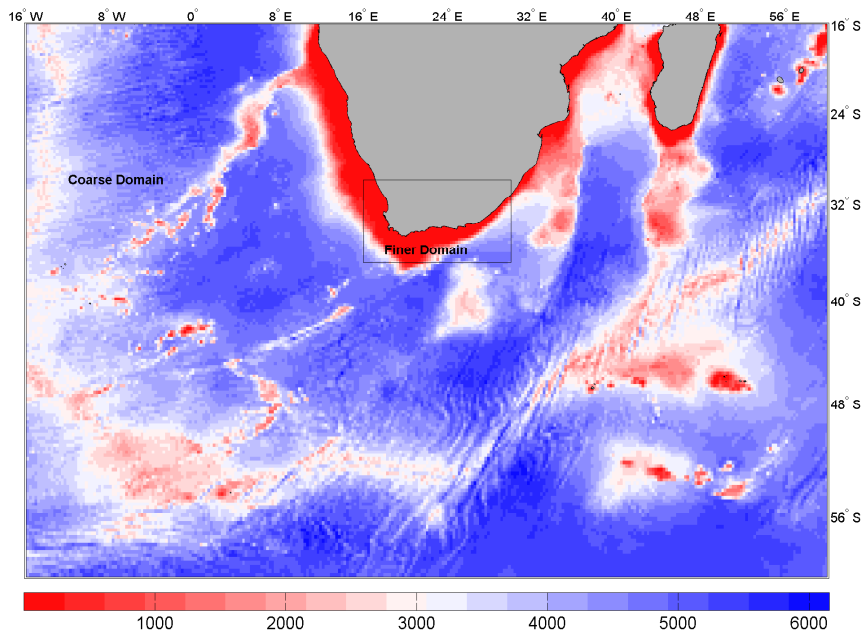
Figure 1.: Domains and meters depth, along the areas of investigation
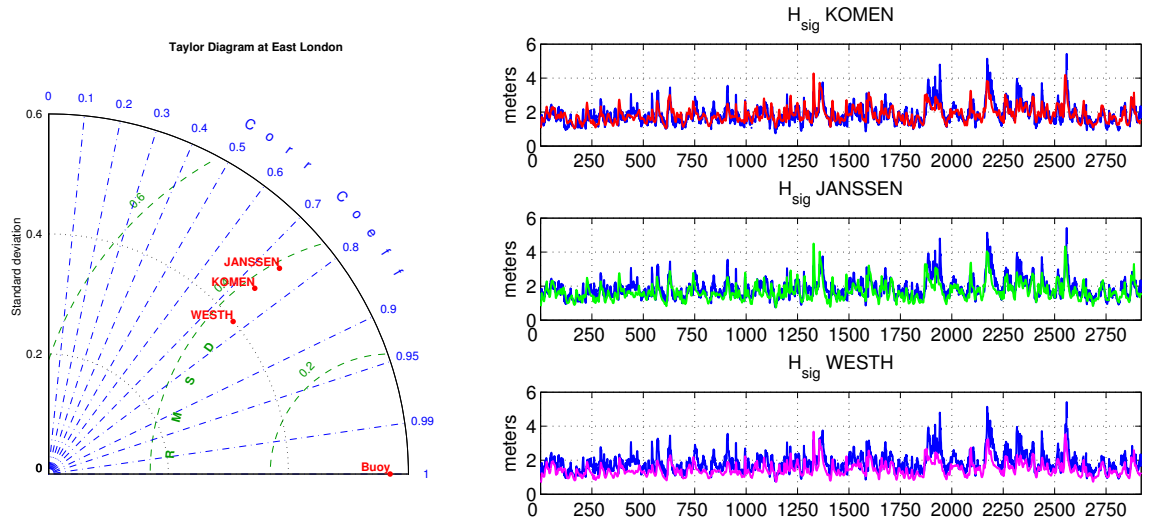
Figure 2.: Taylor diagram for East London and comparison of the generated H_{sig} by the models, blue is the buoy measurements while the colours indicate results by each different scheme. The measurements are taken every 3 hours
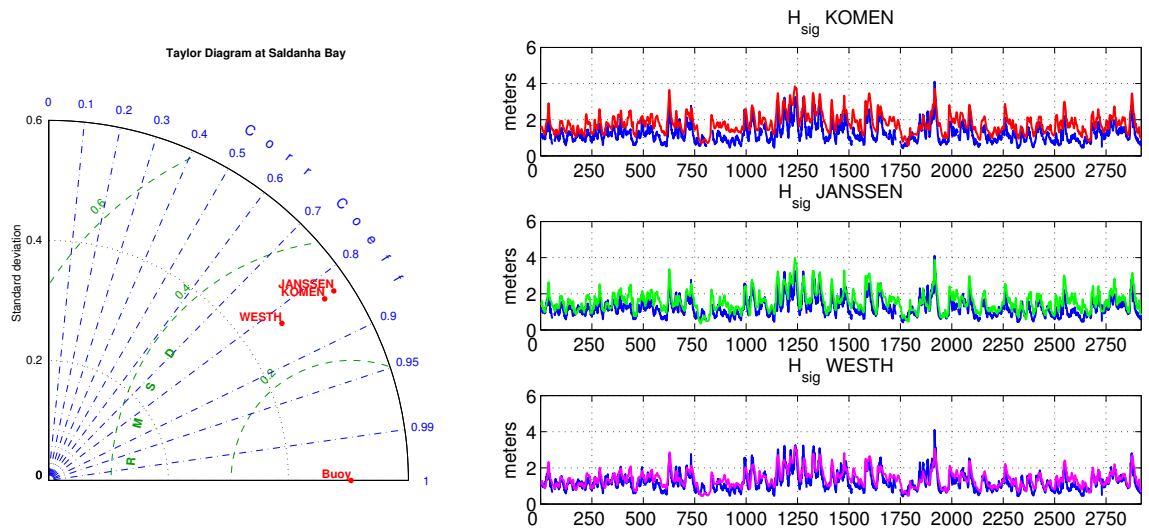
Figure 3.: Taylor diagram for Saldanha Bay and comparison of the generated H_{sig} by the models, blue is the buoy measurements while the colours indicate the results by each different scheme. The measurements are taken every 3 hours

21
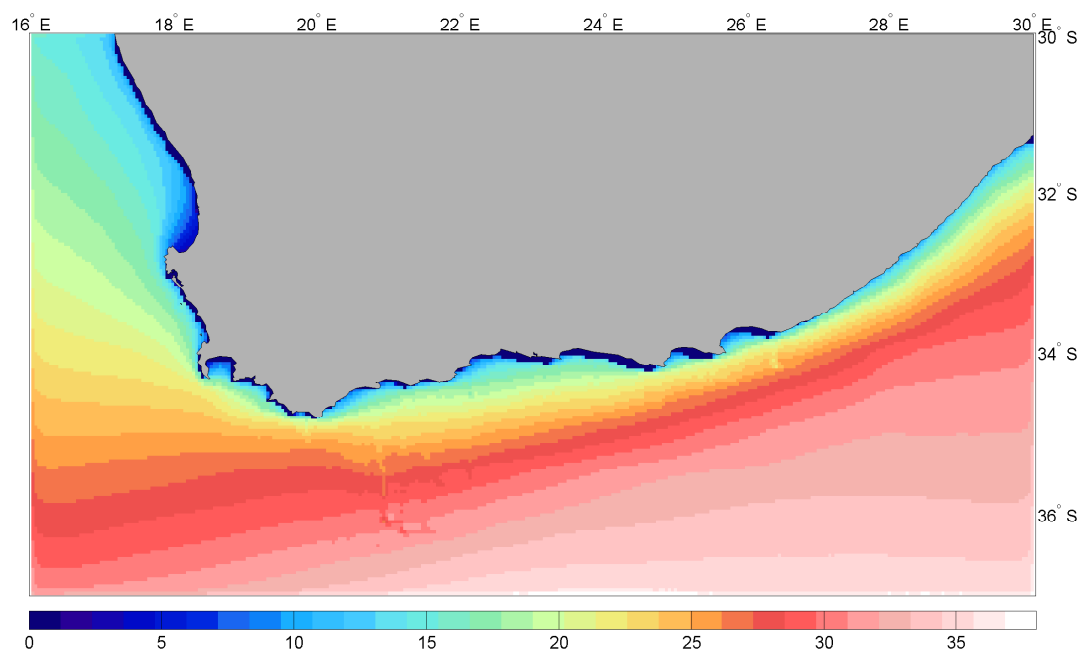
Figure 4.: Overall Wave Energy (kW/m) over the 18 years period (nested domain)

DJF

MAM

23
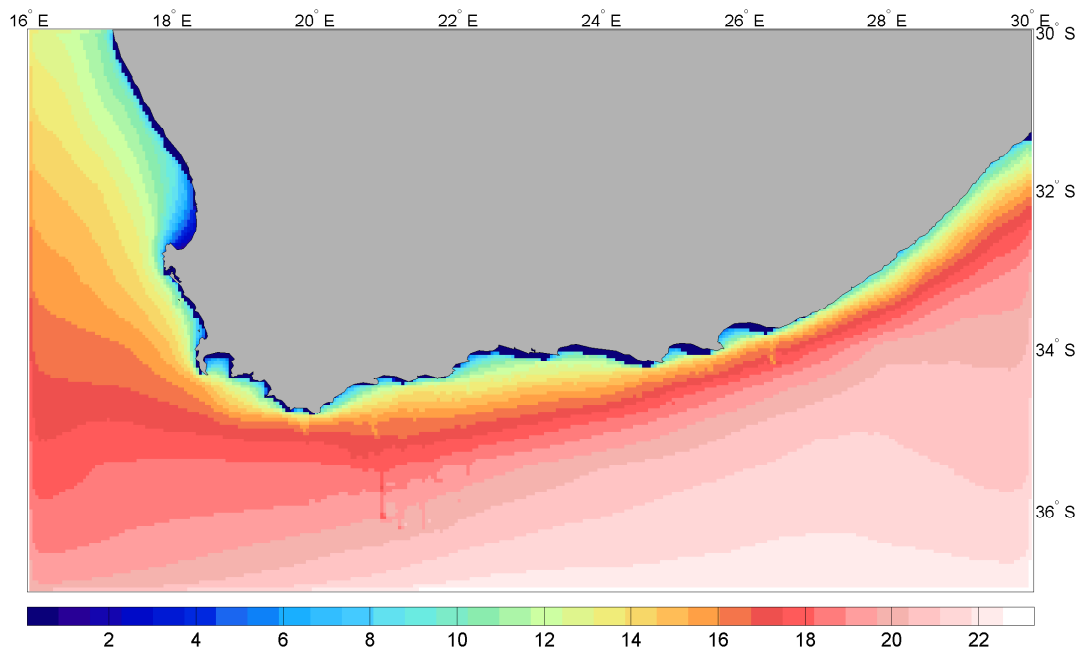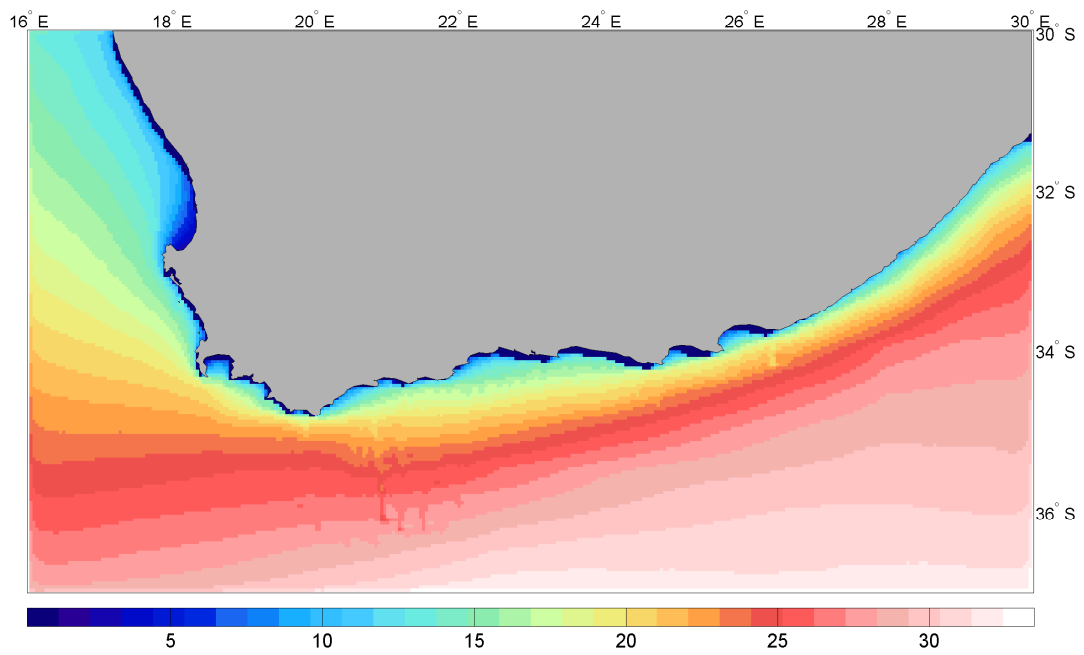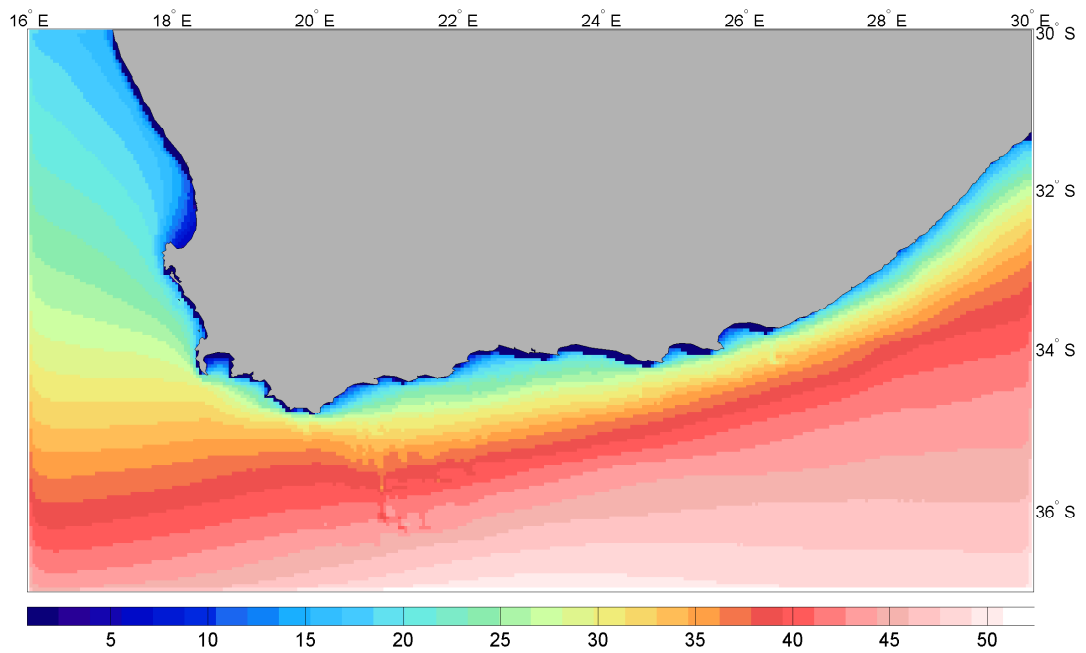
JJA

SON

Figure 5.: Seasonal Wave Power distribution

Figure 6.: Additional Locations Extracted, with corresponding depth (m)

Figure 7.: East London (left panel), Saldanha Bay (right panel) monthly measured wave power from the 2014 recordings by the buoy.

Figure 8.: Annual Mean Wave Power
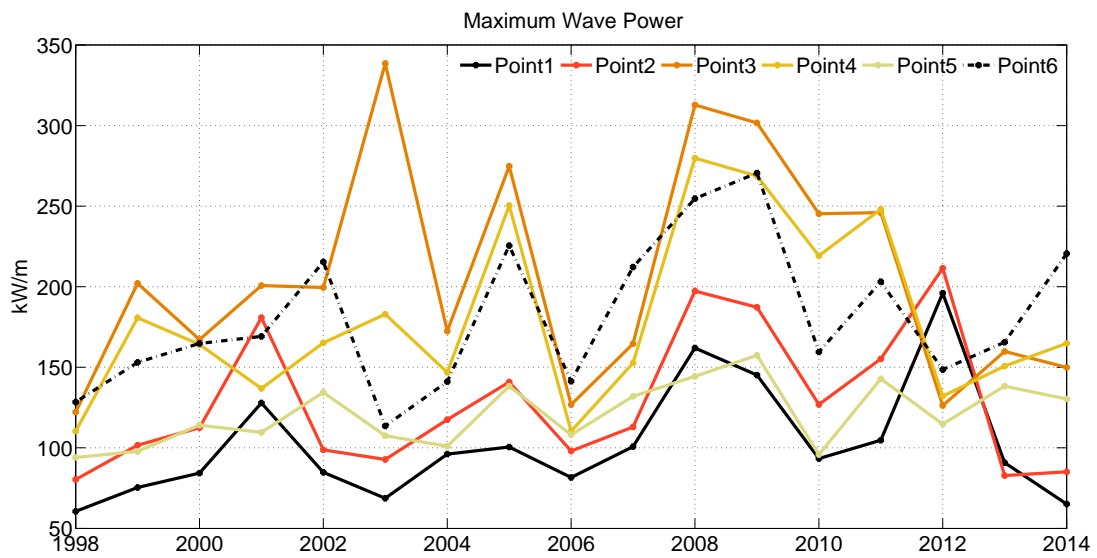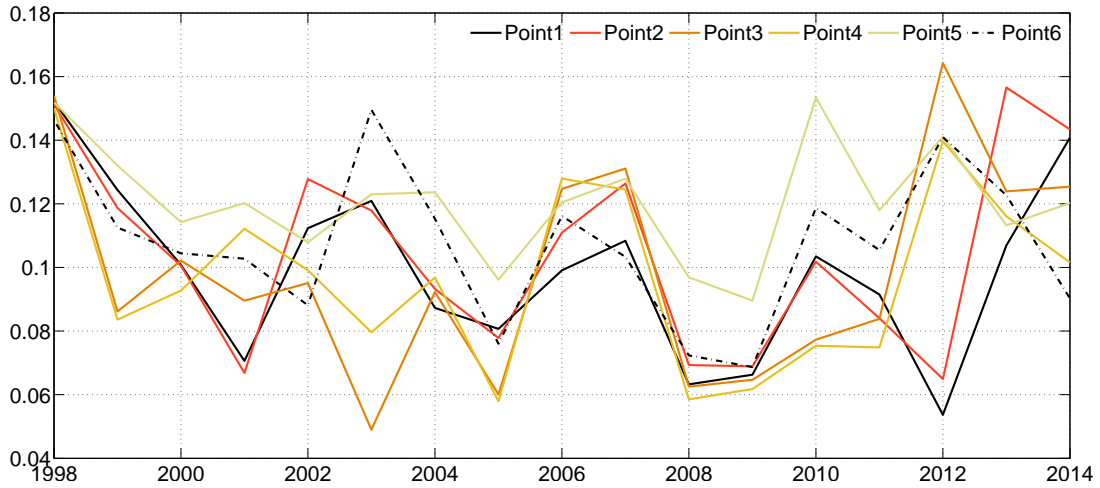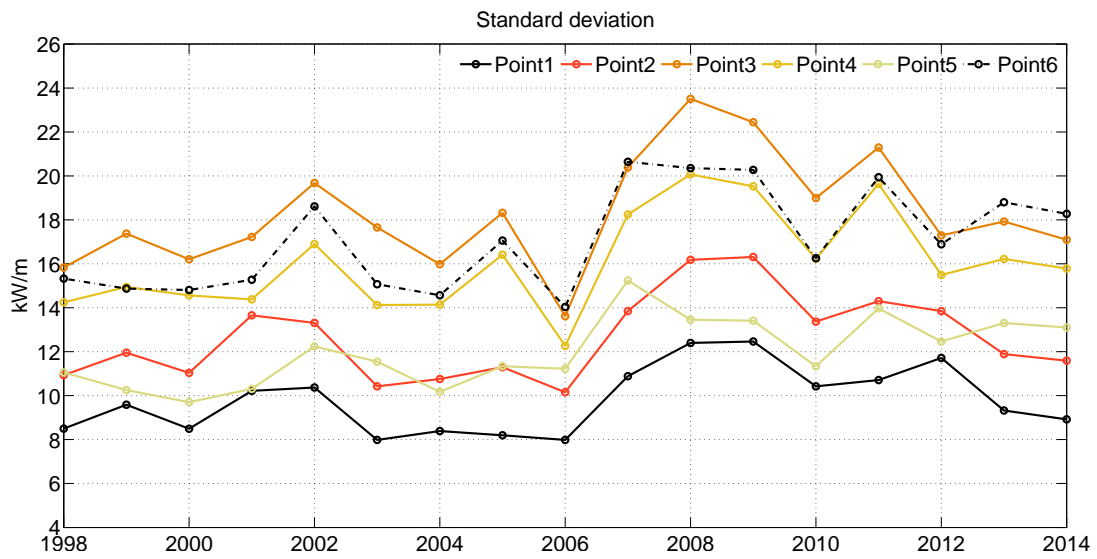

Figure 9.: 99th percentiles for the locations

Figure 10.: Annual Maximum Wave Power Occurrence

Figure 11.: Mean Over Maximum encountered power levels

Figure 12.: Standard deviation

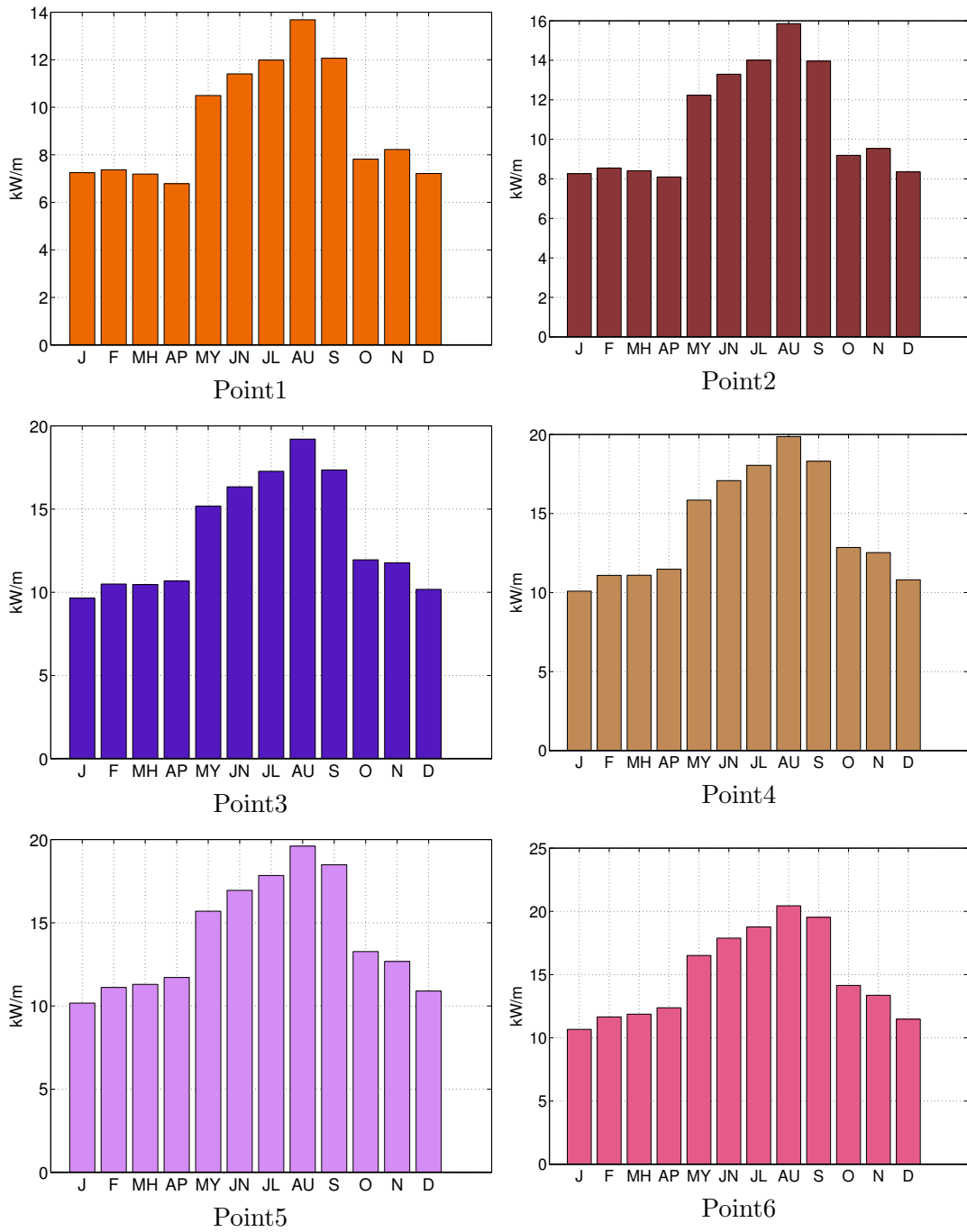Figure 13.: Monthly Wave Power (kW/m) Estimates

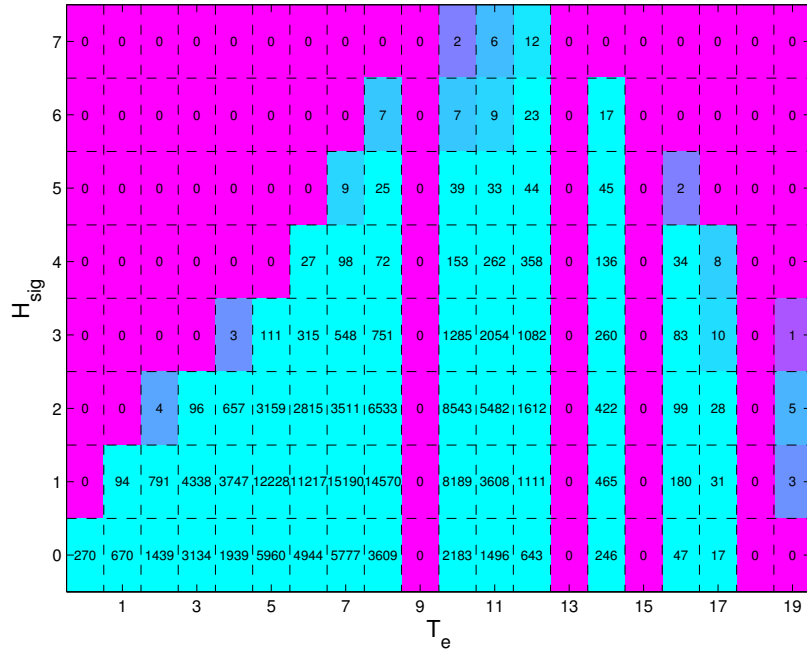Figure 14.: Bivariate H_{sig}-T_e for Point 1
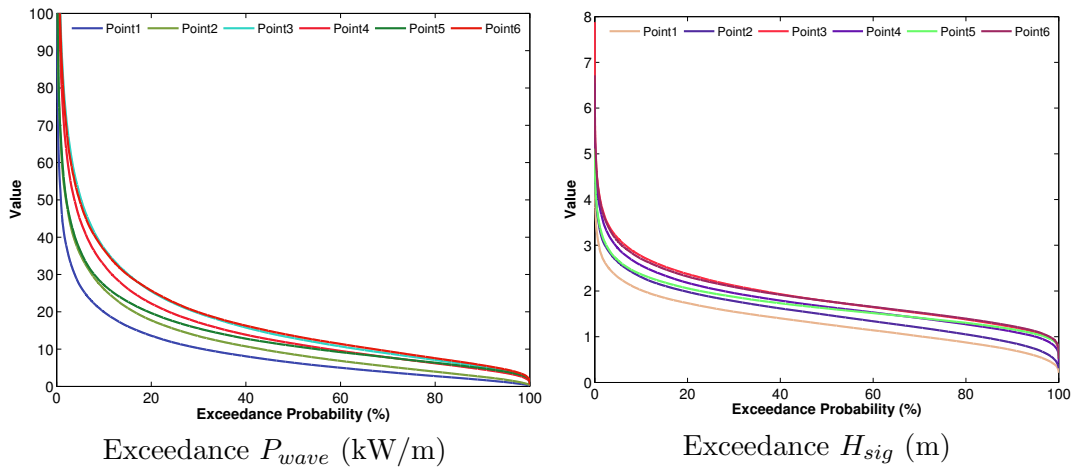

Exceedance P_{wave} (kW/m)

Exceedance H_{sig} (m)

Figure 15.: Exceedance Probabilities